

# Columnar Self-Assembly of $\text{Cu}_2\text{S}$ Hexagonal Nanoplates Induced by Tin(IV)–X Complex as Inorganic Surface Ligand

Xiaomin Li, Huaibin Shen, Jinzhong Niu, Sen Li, Yongguang Zhang, Hongzhe Wang,\* and Lin Song Li\*

Key Laboratory for Special Functional Materials of the Ministry of Education, Henan University, Kaifeng 475004, P. R. China

Received May 9, 2010; E-mail: lsli@henu.edu.cn; whz@henu.edu.cn

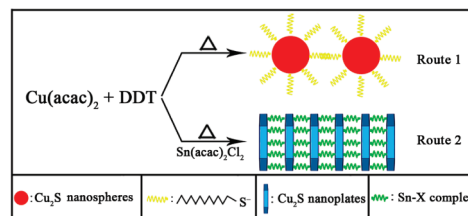
**Abstract:** We have prepared columnar self-assembled  $\text{Cu}_2\text{S}$  hexagonal nanoplates induced by a  $\text{Sn-X}$  complex for the first time and demonstrated that the  $\text{Sn-X}$  complex can affect not only the morphology of the nanocrystals but also the self-assembly ability of the nanocrystals.

The bottom-up colloid chemical synthesis of various inorganic nanocrystals with well-defined size, shape, and composition has achieved great success over the past two decades.<sup>1</sup> Because of their extraordinary physical and chemical properties, colloidal inorganic nanocrystals have shown potential applications in light-emitting devices, photodetectors, solar cells, and other devices.<sup>1</sup> With the further development of synthetic methodologies, the design and construction of nanocrystal superlattices, which is the basis of nanomaterials and nanodevices, has begun to attract great interest in both fundamental and applied research areas.<sup>2</sup> To achieve this goal, the self-assembly technique has been widely used because of its distinct advantages, such as simplicity and low cost. Surface ligands are usually organic compounds with long hydrocarbon chains,<sup>3</sup> and the insulating nature of such organic ligands typically results in very poor interparticle coupling. Most recently, Talapin and co-workers<sup>4</sup> found that various molecular metal chalcogenide complexes (MCCs), such as  $[\text{Sn}_2\text{S}_6]^{4-}$  and  $[\text{Sn}_2\text{Se}_6]^{4-}$ , could serve as convenient ligands for colloidal nanocrystals and nanowires. The MCC ligands behaved as electronically transparent “glue” for nanocrystals. With various special properties, inorganic ligands may open an innovative way to device-level manipulation of MCC-nanocrystals and benefit many nanocrystal-related potential applications. Furthermore, they may also influence the self-assembly ability and morphology of nanocrystals as organic ligands do.

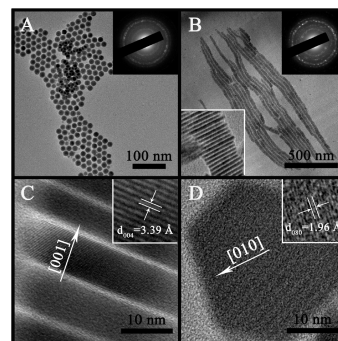
As a p-type semiconductor with a bulk band gap of 1.2 eV, copper(I) sulfide ( $\text{Cu}_2\text{S}$ ) has many applications in solar cells,<sup>1h</sup> cold cathodes,<sup>1i</sup> and nanoscale switches.<sup>1j</sup> In this communication, we report the columnar self-assembly of  $\text{Cu}_2\text{S}$  hexagonal nanoplates induced by a tin(IV) sulfide complex ( $\text{Sn-X}$  complex) that was formed by the reaction between tin(IV) bis(acetylacetonate) dichloride  $[\text{Sn}(\text{acac})_2\text{Cl}_2]$  and excess 1-dodecanethiol (DDT). As shown in Scheme 1, when copper(II) acetylacetonate  $[\text{Cu}(\text{acac})_2]$  reacted with DDT, only DDT-capped  $\text{Cu}_2\text{S}$  nanospheres were synthesized. Columnar self-assembled hexagonal  $\text{Cu}_2\text{S}$  nanoplates were synthesized once  $\text{Sn}(\text{acac})_2\text{Cl}_2$  was involved in the reaction. This indicated that the  $\text{Sn-X}$  complex did play an important role in controlling the shape of the  $\text{Cu}_2\text{S}$  nanocrystals, which further influenced their self-assembly ability.

Figure 1A,B shows transmission electron microscopy (TEM) images of the two different kinds of morphologies of  $\text{Cu}_2\text{S}$  nanocrystals formed without and with the participation of

**Scheme 1.** Synthetic Procedure for  $\text{Cu}_2\text{S}$  Nanospheres and  $\text{Cu}_2\text{S}$  Hexagonal Nanoplates with Columnar Self-Assembly



$\text{Sn}(\text{acac})_2\text{Cl}_2$  in the reaction, respectively. Nearly monodisperse  $\text{Cu}_2\text{S}$  nanospheres were prepared in the absence of  $\text{Sn}(\text{acac})_2\text{Cl}_2$  (also see Figure S1 in the Supporting Information), while the shape of the  $\text{Cu}_2\text{S}$  nanocrystals was totally different when  $\text{Sn}(\text{acac})_2\text{Cl}_2$  was introduced. As shown in Figure 1B, these  $\text{Cu}_2\text{S}$  nanocrystals had a strong self-assembling tendency, and at first glance, one-dimensional (1D) superstructures were formed by the arrays of many nanorods. However, careful observation revealed that the building blocks of the 1D superstructures were in fact hexagonal nanoplates. The areas marked by blue and red rectangles in Figure 2A show upright and tilted hexagonal nanoplates, respectively, and clearly reveal that the 1D superstructures of  $\text{Cu}_2\text{S}$  nanocrystals were composed of hexagonal nanoplates stacking face-to-face. The high-resolution TEM (HRTEM) image of the ordered hexagonal nanoplate arrays standing edge-on perpendicular to the substrate (Figure 1C) shows a lattice spacing of 3.39 Å, which is consistent with the (004)-plane  $d$  spacing of monoclinic primitive  $\text{Cu}_2\text{S}$ . In other words, the nanoplates assembled with their {001} planes perpendicular to



**Figure 1.** (A) TEM images of as-synthesized DDT-capped circular  $\text{Cu}_2\text{S}$  nanospheres synthesized by route 1. The inset shows the selected-area electron diffraction (SAED) pattern. (B) TEM image of as-synthesized  $\text{Cu}_2\text{S}$  nanoplates with columnar self-assembly synthesized by route 2. The insets show the SAED pattern and a high magnification of the selected area. (C) HRTEM image of the ordered hexagonal nanoplate arrays standing edge-on perpendicular to the substrate. (D) HRTEM image of a hexagonal nanoplate lying flat on the substrate.

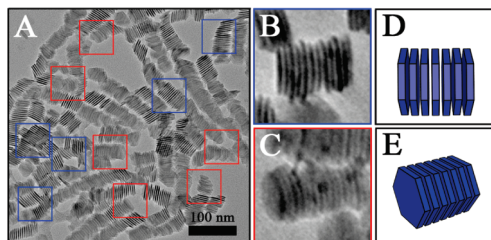


**Figure 2.** (A) TEM images of typical  $\text{Cu}_2\text{S}$  nanoplates with columnar self-assembly synthesized by route 2 at 200 °C for 30 min. Blue and red rectangles indicate the upright and tilted hexagonal nanoplates, respectively. (B, C) High-magnification TEM images and (D, E) illustrations of the upright and tilted hexagonal nanoplates.

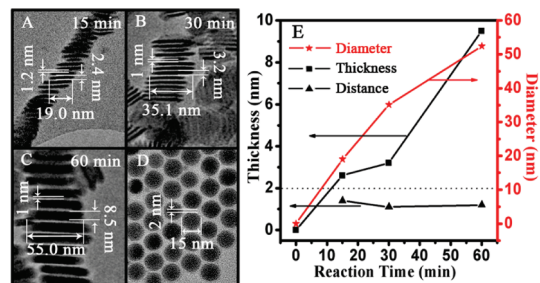


**Figure 3.** Feature TEM images of (A–C) typical columnar self-assembly of hexagonal  $\text{Cu}_2\text{S}$  nanoplates synthesized by route 2 at different reaction times and (D)  $\text{Cu}_2\text{S}$  nanospheres synthesized by route 1. (E) Evolution of the diameter (red ★) and thickness (black ■) of the  $\text{Cu}_2\text{S}$  nanoplates and the distance between two adjacent face-to-face nanoplates (black ▲).

the substrate, which is in agreement with the literature.<sup>5</sup> Figure 1D shows an HRTEM image of a single hexagonal nanoplate lying flat on its hexagonal facet. It can be seen that the lattice spacing is 1.96 Å, corresponding to the (080)-plane  $d$  spacing of monoclinic primitive  $\text{Cu}_2\text{S}$ . Upon adjustment of the experimental parameters, the as-synthesized  $\text{Cu}_2\text{S}$  hexagonal nanoplates self-assembled into large-scale 1D and 3D columns (Figures S2–S4).

Further experiments revealed that the size of the 1D-superstructured hexagonal  $\text{Cu}_2\text{S}$  nanoplates could be tuned simply by changing the reaction time (Figure 3 and Figure S5). When the reaction time was 15 min, the platelet particles had an average diameter of 19 nm with an average thickness of 2.4 nm. Superstructures were still maintained after 60 min of reaction, while the diameter and thickness of hexagonal nanoplates were increased to ~55 nm and ~9.5 nm, respectively. Even though the particle size grew larger with prolonged reaction time, the distance between two adjacent face-to-face stacked nanoplates kept a fixed value (~1.0 nm). This value was much smaller than that of DDT-capped circular  $\text{Cu}_2\text{S}$  nanospheres, whose average spacing was ~2 nm (Figure 3D), which is consistent with the literature and theoretical values ( $1.9 \text{ nm} < d < 3.8 \text{ nm}$ ).<sup>2d,6,7</sup> In comparison with the interparticle spacing of DDT-capped circular  $\text{Cu}_2\text{S}$  nanospheres, the ligands capping the hexagonal nanoplates should be shorter ligands related to the Sn–X complex on the basis of the analysis from FTIR, XPS, and UV–vis spectra (Figures S6–S8). The electric transport properties of  $\text{Cu}_2\text{S}$  nanocrystals with and without the participation of the Sn–X complex were also studied (Figure S9). The as-synthesized DDT-capped nanocrystals showed low conductivity as a result of the large interparticle spacing (~2.0 nm) connected by the insulating DDT molecules. The conductivity of the self-assembled nanoplates, however, was improved nearly 1 order of magnitude because of the short interparticle spacing (~1.0 nm) linked by the Sn–X complex.

According to the results of control experiments and characterizations, we assume that there are two main probabilities resulting in the columnar assembly: first, in accordance with the literature,<sup>5</sup> the platelet shape of the nanocrystals may easily lead to the formation of columnar assemblies; second, the Sn–X complex should have a special structure whose two ends could both bind to the surface of hexagonal nanoplates, so the nanoplates could stack face-to-face and form a columnar self-assembled structure. Similar results could also be observed when other Sn(IV) salts (such as  $\text{SnCl}_4$ ) were used (Figure S10). According to literature reported by Talapin,<sup>4</sup> the Sn–X complex in the form of  $[\text{Sn}_2\text{S}_6]^{4-}$  is proposed, as shown in Scheme 1 (green ligands); however, an in-depth investigation of the exact structure of the Sn–X complex is still in progress.

In summary, we have prepared columnar self-assembled  $\text{Cu}_2\text{S}$  hexagonal nanoplates induced by a Sn–X complex for the first time and demonstrated that the Sn–X complex can affect not only the morphology of the nanocrystals (as traditional organic ligands do) but also the self-assembly ability of the nanocrystals. We believe that the methodology of constructing self-assembled nanostructures reported in this communication may turn over a new leaf in device-level manipulation of nanocrystals and many nanocrystal-related potential applications.

**Acknowledgment.** This work was supported by the research project of the National Natural Science Foundation of China (20771035), Program for New Century Excellent Talents in University of Chinese Ministry of Education, the Hi-Tech Research and Development Program of China (863 Plan, 2006AA03Z3592), and Innovation Scientists and Technicians Troop Construction Projects of Henan Province.

**Supporting Information Available:** Experimental details, results and discussion on  $\text{Cu}_2\text{S}$  nanospheres, and 1D and 3D columnar self-assembly of hexagonal  $\text{Cu}_2\text{S}$  nanoplates and Sn–X complexes. This material is available free of charge via the Internet at <http://pubs.acs.org>.

## References

- (1) (a) Brus, L. J. *Phys. Chem.* **1986**, *90*, 2555–2560. (b) Murray, C. B.; Kagan, C. R.; Bawendi, M. G. *Annu. Rev. Mater. Sci.* **2000**, *30*, 545–610. (c) Alivisatos, A. P. *Science* **1996**, *271*, 933–937. (d) Chan, W. C. W.; Nie, S. M. *Science* **1998**, *281*, 1616–1618. (e) Huynh, W. U.; Dittmer, J. J.; Alivisatos, A. P. *Science* **2002**, *295*, 2425–2427. (f) Sun, Q. J.; Wang, Y. A.; Li, L. S.; Wang, D. Y.; Zhu, T.; Xu, J.; Yang, C. H.; Li, Y. F. *Nat. Photonics* **2007**, *1*, 717–722. (g) Fan, H. *Chem. Commun.* **2008**, 1383–1394. (h) Wu, Y.; Wadia, C.; Ma, W.; Sadler, B.; Alivisatos, A. P. *Nano Lett.* **2008**, *8*, 2551–2555. (i) Chen, J.; Deng, S. Z.; Xu, N. S.; Wang, S. H.; Wen, X. G.; Yang, S. H.; Yang, C. L.; Wang, J. N.; Ge, W. K. *Appl. Phys. Lett.* **2002**, *80*, 3620–3622. (j) Chen, L.; Xia, Y. D.; Liang, X. F.; Yin, K. B.; Yin, J.; Liu, Z. G.; Chen, Y. *Appl. Phys. Lett.* **2007**, *91*, 073511.
- (2) (a) Lu, W.; Liu, Q.; Sun, Z.; He, J.; Ezeolu, C.; Fang, J. *J. Am. Chem. Soc.* **2008**, *130*, 6983–6991. (b) Shevchenko, E. V.; Talapin, D. V.; Murray, C. B.; O'Brien, S. *J. Am. Chem. Soc.* **2006**, *128*, 3620–3637. (c) Baker, J. L.; Widmer-Cooper, A.; Toney, M. F.; Geissler, P. L.; Alivisatos, A. P. *Nano Lett.* **2010**, *10*, 195–201. (d) Bigioni, T. P.; Lin, X. M.; Nguyen, T. T.; Corwin, E. I.; Witten, T. A.; Jaeger, H. M. *Nat. Mater.* **2006**, *5*, 265–270.
- (3) Lu, C.; Chen, Z.; O'Brien, S. *Chem. Mater.* **2008**, *20*, 3594–3600.
- (4) Kovalenko, M. V.; Scheele, M.; Talapin, D. V. *Science* **2009**, *324*, 1417–1420.
- (5) (a) Zhuang, Z.; Peng, Q.; Zhang, B.; Li, Y. *J. Am. Chem. Soc.* **2008**, *130*, 10482–10483. (b) Sigman, M. B.; Ghezelsb, A.; Hanrath, T.; Saunders, A. E.; Lee, F.; Korgel, B. A. *J. Am. Chem. Soc.* **2003**, *125*, 16050–16057. (c) Larsen, T. H.; Sigman, M.; Ghezelsb, A.; Doty, R. C.; Korgel, B. A. *J. Am. Chem. Soc.* **2003**, *125*, 5638–5639. (d) Saunders, A. E.; Ghezelsb, A.; Smilgies, D. M.; Sigman, M. B.; Korgel, B. A. *Nano Lett.* **2006**, *6*, 2959–2963.
- (6) (a) Talapin, D. V.; Lee, J. S.; Kovalenko, M. K.; Shevchenko, E. V. *Chem. Rev.* **2010**, *110*, 389–458. (b) Courty, A. *J. Phys. Chem. C* **2010**, *114*, 3719–3731.
- (7) Bain, C. D.; Evall, J.; Whitesides, G. M. *J. Am. Chem. Soc.* **1989**, *111*, 7155–7164.

JA103955S